

Low compressible BP_3N_6

George S. Manyali^{1,2,3,*} and James Sifuna^{1,4,5}

¹*Computational and Theoretical Physics Group, 190-50100, Kakamega, Kenya.*

²*Department of Physics, Masinde Muliro University of Science and Technology, 190-50100, Kakamega, Kenya*

³*Department of Physical sciences, Kaimosi Friends University College, 385-50309, Kaimosi, Kenya*

⁴*Department of Natural Sciences, The Catholic University of Eastern Africa, 62157 - 00200, Nairobi, Kenya*

⁵*Materials Modeling Group, Department of Physics and Space Sciences,*

The Technical University of Kenya, 52428-00200, Nairobi, Kenya

(Dated: September 23, 2019)

Using first principles calculation, the structural and mechanical properties of BP_3N_6 which adopts an orthorhombic structure with space group Pna2₁ (no. 33), were determined at three different pressure values (0, 20 and 42.4 GPa). The nine independent elastic constants meet all necessary and sufficient conditions for mechanical stability criteria for an orthorhombic crystal. BP_3N_6 show strong resistance to volume change hence a potential low compressible material. The Vicker's hardness of BP_3N_6 was found to range between 49-51 GPa for different external pressures imposed on the crystal. These high values of Vicker's hardness implies that BP_3N_6 is a potential superhard material.

I. INTRODUCTION

Hardness is an important property that determines many of the technological applications of materials¹. Designing materials based on first principles approach, synthesize and then characterization of these materials is of great interest to both theoretical and experimental material scientists. Well known superhard materials such as diamond and boron nitride display strong covalent bonds, low compressibility and high wear resistance. Applicability of these materials at high-pressure is limited and therefore there is need for new materials that would work perfectly in those harsh conditions. For many years now search for new superhard materials has been an order of the day. This search is unlikely to end any time soon due to the fact that diamond remains to be the hardest known material made of a single light element called carbon. Combination of carbon and other light elements such as nitrogen have shown promising results from the theoretical perspective²⁻⁶ but most of the predicted materials have not been realized experimentally.

The present study has been prompted by the recent explorative investigation of phosphorus nitrides by Vogel *et.al.*^{7,8} who synthesized a high-pressure polymorph of boron phosphorus nitride ($\beta\text{-BP}_3\text{N}_6$). This phase adopts an orthorhombic structure with space group Pna2₁ (no. 33). The $\beta\text{-BP}_3\text{N}_6$ phase is characterized with octahedral coordinated phosphorous (P) atoms in a distorted hexagonal closed-packing of nitride anions. This phase was obtained at high-pressure experiment having transformed from $\alpha\text{-BP}_3\text{N}_6$ at a pressure of about 42 GPa. To our knowledge, no previous first-principles calculations have been carried out to investigate the mechanical stability and the hardness of this new phase of $\beta\text{-BP}_3\text{N}_6$ at different pressure.

Mechanical stability is a concept based the elastic constants of a single crystal sample of a material. The elastic constants determine the response of the crystal to external forces that can be characterized in forms of bulk

modulus, shear modulus, Youngs modulus, and Poissons ratio. All these properties can be obtained from density functional theory (DFT)^{9,10} which has become an essential tool for designing novel superhard materials .

In this paper, we first bench marked our study with previous theoretical studies on the lattice parameters, elastic constants, bulk and shear moduli of a hypothetical superhard carbon mononitride (Pnnm-CN)². This compound adopts an orthorhombic crystal structure of space group Pnnm (no. 58) and its Vicker's hardness has been predicted to be above 60 GPa. Once satisfied with Pnnm-CN results we went ahead to investigate the lattice parameters, elastic constants, bulk modulus, shear modulus, Poisson's ratio, Youngs modulus, Vicker's hardness and mechanical stability of BP_3N_6 at different pressure. Both Pnnm-CN and BP_3N_6 adopts an orthorhombic structure with dense network of covalent bonds which are precursors for low compressibility.

The remaining parts of this paper are arranged as follows: in section II, we give a brief outline of the computational details. Results are shown and discussed in section III. Finally in section IV, we provide a conclusion.

II. COMPUTATIONAL DETAILS

Calculations in the present work were performed using Density Functional Theory (DFT)^{9,10} within the Perdew-Burke Ernzerhof (PBE)¹¹ generalized gradient approximation and plane waves basis sets as implemented in the Quantum ESPRESSO package¹². All pseudopotentials were obtained from the pslibrary1.0 maintained by Dal Corso¹³. The cell volume and ions were optimized at three different pressure values i.e 0 GPa, 20 GPa and 42.4 GPa. The k-point sampling¹⁴ was performed on 6x4x4 grid while the kinetic energy cut-off was set to 43 Ry. It is well known that PBE functional overestimates the lattice parameter and consequently affects not only the volume and the density of the compound but also

the mechanical properties of the compound. An external pressure exerted on the crystal structure has also profound influence on the mechanical properties. Therefore, to get physically meaningful results from the calculations of elastic constants, we did not allow the ions to relax. This was necessary to maintain the strain on each ions at different pressure. The thermo_pw package^{15,16} was used to run the elastic constants calculations.

III. RESULTS AND DISCUSSION

A. Physical properties of Pnm-CN at zero pressure

In Table I we have listed calculated physical properties of Pnm-CN at zero pressure predicted using PBE functional. The calculated lattice constants produced from fitting total energy as a function of volume to Murnaghan¹⁷ equation of state are compared to the corresponding theoretical results. In general, our calculated lattice constants and other properties shown in Table I are in agreement with results of previous studies. This results gave us confidence to study lattice parameters a (Å), b (Å), c (Å), volume V (Å³) and density ρ (g/cm³) of BP₃N₆ at zero and elevated pressures.

B. Structural properties of BP₃N₆

Fig. 1 shows the crystal structure of the primitive cell of BP₃N₆ where P are the large atoms labeled as P1, B are medium-size atoms labeled as B1, whereas the smaller ones are N atoms labeled as N1. The unit cell of contains 40 atoms and has a space group of Pna2₁ (no. 33).

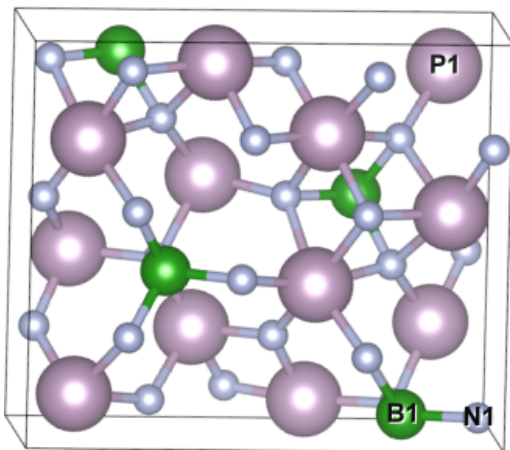


FIG. 1. The crystal structure of the primitive cell of BP₃N₆, where P are the large atoms labeled P1, B are medium-size atoms labeled B1, whereas the smaller ones are N atoms labeled N1. The unit cell of contains 40 atoms and has a space group of Pna2₁ (no. 33).

Table II show the response of lattice parameter to different external pressure exerted on BP₃N₆. As the exerted pressure increase from zero to 20 GPa, the unit-cell contract by 1.87%, 2.04% and 1.79% in a , b and c axes respectively. We see a lot more contraction in b axis than in both a and c axes. This is a clear indication of existence of different bonding behavior along the axes. One would expect strong covalent bonding between boron and nitrogen atoms and weaker bonding character in phosphorus-nitrogen bond formation. On increasing external pressure to 42.4 GPa, the unit-cell contract by 3.51%, 3.78% and 3.39% in a , b and c axes respectively. Again, the b axes display slightly more collapse in its distance than in both a and c axes. At 42.4 GPa, the calculated results are compared with corresponding experimental data from Vogel *et. al.*⁸. It is well known that PBE functional overestimate the lattice constants and consequently the volume of the crystal structure. In this case, the predicted volume of BP₃N₆ is slightly higher that experimental values by 3.5%. Furthermore, volumetric density of a material changes linearly with pressure and inversely with volume. At 42.4 GPa, the predicted density is lower than experimental value by 165 gmm⁻³. Generally, a good agreement is reached between computed and measured values.

C. Elastic stability of BP₃N₆

Since 1954, the work of Born¹⁸ has been used to evaluate elastic stability of crystal structures. The cubic crystals are easy to handle due their high symmetry. Efforts to apply the Born¹⁸ elastic stability criteria on lower symmetry crystals is reported in works of Ravindran *et. al.* and that of Mouhat and co-author^{19,20}. These authors gave a precise description of the form it should take for lower symmetry crystal classes. They^{19,20} particularly considered orthorhombic crystal structure as one such system with lower symmetry. They described it as having nine independent elastic constants namely: C_{11} , C_{12} , C_{13} , C_{22} , C_{23} , C_{33} , C_{44} , C_{55} and C_{66} . The mechanical stability of such orthorhombic crystal is achieved whenever the elastic constants satisfy the following necessary and sufficient conditions as prescribed by Born¹⁸:

$$\begin{aligned}
 C_{11} &> 0 \\
 C_{11}C_{22} &> C_{12}^2 \\
 C_{11}C_{22}C_{33} + 2C_{12}C_{13}C_{23} - C_{11}C_{23}^2 - C_{22}C_{13}^2 - C_{33}C_{12}^2 &> 0 \\
 C_{44} &> 0 \\
 C_{55} &> 0 \\
 C_{66} &> 0
 \end{aligned} \tag{1}$$

More work on orthorhombic crystal system has been illustrated by Wen *et. al.*²¹. These particular authors applied elastic stability conditions shown in Eq. (1) on orthorhombic TiAl alloy. They underscored the usefulness of Eq. (1) in checking stability of orthorhombic crystal

TABLE I. Equilibrium structural parameters a (Å), b (Å), c (Å), elastic constants (GPa), bulk modulus (B), shear modulus G, G/B ratio and Vickers hardness (H_v) in GPa of Pnnm-CN calculated at zero pressure.

Pressure	a	b	c	C_{11}	C_{22}	C_{33}	C_{44}	C_{55}	C_{66}	C_{12}	C_{13}	C_{23}	B	G	G/B	H_v
This work 0	5.340	3.955	2.376	499.2	635.8	1172.2	420.5	274.2	368.7	178.2	74.9	138.9	328.7	322.6	0.98	54.4
Others ²	5.335	3.952	2.374	506	643	1183	442	275	372	191	80	140	336	326	0.97	62.5

TABLE II. Lattice parameters a (Å), b (Å), c (Å), volume V (Å³) and density ρ (g/cm³) of BP₃N₆ space group Pna2₁ (no. 33) calculated at different pressures in GPa.

	pressure	a	b	c	V	ρ
This work	0	4.212	7.789	9.063	297.3	4.193
	20	4.133	7.630	8.900	280.7	4.442
	42.4	4.064	7.494	8.755	266.6	4.676
Expt. ⁸	42.4	4.0115	7.411	8.666	257.65	4.841

system.

In this work, the calculated values of the nine independent elastic constants at different values of pressure (0, 20 and 42.4 GPa) are listed in the Table III and they satisfy the necessary and sufficient conditions prescribed for an orthorhombic system. All nine independent elastic constants increases monotonically with pressure. Already at zero pressure, BP₃N₆ depicts a material with large elastic constants which has a strong correlation with compressibility and hardness of a material. At elevated pressure, shorter covalent bonds will resist change in volume, a response that can be captured as enhanced elastic constants. At 42.4 GPa, BP₃N₆ has very large elastic constants comparable to that of diamond. We anticipate such large elastic constants will attract wide industrial application of BP₃N₆ and where possible a substitute to already existing hard materials. It is noted that computing properties of a low symmetry system is tricky and therefore one has to be careful with the values of C_{11} , C_{12} , C_{13} , C_{22} , C_{23} , C_{33} , C_{44} , C_{55} and C_{66} as will always depend on the orientation of the unit cell. To our knowledge, there is no data on elastic constants to compare with our results and hence our work lays a foundation for future references.

From the single crystal elastic constants data²¹, the polycrystalline bulk modulus B and shear modulus G can be calculated by using the Voigt approximation²²; which describes the upper bound and the Reuss approximation²³ that describes the lower bound. The Average of the two bounds is often described by the Hills approximation²⁴. Below are equations that relates the nine independent elastic constants to B_V and G_V in Voigt notation, whereas B_R and G_R represent Reuss notations.

$$B_V = (C_{11} + 2C_{12} + 2C_{13} + C_{22} + 2C_{23} + C_{33})/9 \quad (2)$$

$$G_V = (C_{11} - C_{12} - C_{13} + C_{22} - C_{23} + C_{33} + 3C_{44} + 3C_{55} + 3C_{66})/15 \quad (3)$$

$$\chi = C_{13}(C_{12}C_{23} - C_{13}C_{22}) + C_{23}(C_{12}C_{13} - C_{23}C_{11}) + C_{33}(C_{11}C_{22} - C_{12}^2)$$

$$B_R = \chi(C_{11}(C_{22} + C_{33} - 2C_{23}) + C_{22}(C_{33} - 2C_{13}) - 2C_{33}C_{12} + C_{12}(2C_{23} - C_{12}) + C_{13}(2C_{12} - C_{13}) + C_{23}(2C_{13} - C_{23}))^{-1} \quad (4)$$

$$G_R = 15(4(C_{11}(C_{22} + C_{33} + C_{23}) + C_{22}(C_{33} + C_{13}) + C_{33}C_{12} - C_{12}(C_{23} + C_{12}) - C_{13}(C_{12} + C_{13}) - C_{23}(C_{13} + C_{23}))/\chi + 3(1/C_{44} + 1/C_{55} + 1/C_{66}))^{-1} \quad (5)$$

For simplicity, the averages of Voigt and Reuss approximations are presented as B and G for bulk and shear moduli respectively.

$$B = \frac{B_V + B_R}{2} \quad (6)$$

$$G = \frac{G_V + G_R}{2} \quad (7)$$

The derived quantities from B and G are presented as Young's modulus (E) and Poisson's ratio (n).

$$E = \frac{9BG}{3B + G} \quad (8)$$

The Young's modulus is a measures for stiffness of a material while Poisson's ratio is often used to classify materials as either ductile or brittle²⁵. This concept by Haines *et. al.* will normally treat a brittle material as one having n below 0.33 while a ductile material as one that has n greater than 0.33.

$$n = \frac{3B - 2G}{6B + 2G} \quad (9)$$

TABLE III. Elastic constants in GPa of BP₃N₆ calculated at different pressures.

	Pressure	C_{11}	C_{22}	C_{33}	C_{44}	C_{55}	C_{66}	C_{12}	C_{13}	C_{23}
BP ₃ N ₆	0	818.3	720.1	788.6	296.9	302.5	306.8	97.0	87.0	141.4
	20	972.5	876.2	943.9	345.1	360.6	367.4	164.2	151.5	198.6
	42.4	1103.0	1009.3	1073.1	385.2	409.5	419.1	224.1	208.1	248.4

On the other hand, Pugh's²⁶ definition of a ductile/brittle material is based on the G/B ratio. Ductility is measured as a value of G/B less than 0.5, while a material is rated brittle if G/B goes beyond 0.5. Superhard phases of hypothetical C_3N_4 and diamond are good examples of brittle materials as demonstrated in the previous work of this author⁴.

For this work, the calculated bulk modulus (B), shear modulus (G), Young's modulus (E), and Poisson's ratio (n) of BP₃N₆ in Voigt's and Reuss's approaches are listed in Table IV. The bulk modulus which is also referred to as incompressibility, is a ratio that relates an applied constant stress to the fractional volumetric change. BP₃N₆ has a bulk modulus of about 330 GPa comparable to many other low-compressible compounds such as SiO₂ with bulk modulus of 305 GPa, HfN with bulk modulus of 306 GPa, OsB₂ with bulk modulus of 297 GPa²⁷⁻³⁰. The low compressibility of BP₃N₆ can be attributed to highly condensed network built up from the tetrahedra BN₄ and octahedra PN₆ coordination. Although it has been argued that incompressibility is a good indicator of hardness of a material, it is the shear modulus that is strongly associated with hardness. The shear modulus relates to how a material responds to change in shape at constant volume. Calculated shear modulus of BP₃N₆ is about 313 GPa and is in the same range as that of Pnnm-CN reported as 322 GPa, see Tables IV and II respectively. The current value of shear modulus (313 GPa) do not compete that of diamond (546 GPa) as reported elsewhere^{3,4}. It is worth noting that shear modulus increases with increasing pressure. This implies that a material has high resistance to shape change when it is under the influence of an external pressure. As indicated earlier, Young's modulus is a measure for stiffness of a material. It is derived from both shear and bulk moduli. Computed values of BP₃N₆'s Young's moduli for different pressure are presented in Tables IV. The calculated Poisson's ratio suggests that BP₃N₆ should be classified as a brittle material since the value of n is less than 0.33 even at high pressure. Similarly, the G/B ratio calculated as 0.94 at zero pressure, 0.86 at 20 GPa and 0.81 at 42.4 GPa predicts BP₃N₆ as a brittle material with G/B greater than 0.5. The values of B/G for BP₃N₆ are shown in Table V. There is a tendency of BP₃N₆ to transform from brittleness to ductility when exposed to extremely high pressure as depicted by diminishing G/B ratio at elevated pressure. This trend can also be interpreted to mean that BP₃N₆ will undergo pressure-induced phase transformation to lower symmetry crystal structures such as triclinic at extremely high

pressures. Isotropy of crystal structure is very critical in characterization of any compound. The single crystal shear anisotropy factors $A_{\{100\}}$ in $\{100\}$ planes, $A_{\{010\}}$ in $\{010\}$ planes, and $A_{\{001\}}$ in $\{001\}$ planes are defined as²⁰

$$A_{\{100\}} = 4C_{44}/(C_{11} + C_{33}2C_{13}), \quad (10)$$

$$A_{\{010\}} = 4C_{55}/(C_{22} + C_{33}2C_{23}), \quad (11)$$

$$A_{\{001\}} = 4C_{66}/(C_{11} + C_{22} - 2C_{12}). \quad (12)$$

The percentage anisotropy in compressibility A_B and shear A_G is defined as³¹

$$A_B = \frac{B_V - B_R}{B_V + B_R}, A_G = \frac{G_V - G_R}{G_V + G_R}. \quad (13)$$

A zero value of A_B and A_G corresponds to elastic isotropy, while a value of 100% corresponds to the largest possible anisotropy. The universal anisotropy index (A^U) is defined as³²

$$A^U = \frac{B_V}{B_R} + \frac{5G_V}{G_R} - 6. \quad (14)$$

A nonzero value of A^U is a measure of the anisotropy. The shear anisotropy factors ($A_{\{100\}}, A_{\{010\}}, A_{\{001\}}$), percent anisotropy factors of bulk (A_B) and shear (A_G) moduli, and universal anisotropy factor A^U of BP₃N₆ are presented in Table V. For isotropic case, we expect A_B, A_G and A^U to be zero and any deviation from zero is a clear indicator for anisotropy. Therefore, BP₃N₆ is anisotropic with highest deviations observed in both $A_{\{100\}}$ and $A_{\{001\}}$ directions. The $A_{\{100\}}$ direction is more isotropic than other directions. In the introduction of this article, it was stated clearly that hardness is an important property that determines many of the technological applications of materials¹. The Vicker's hardness in this work was estimated on the basis of the so called Chen model³⁰ that has been widely used to predict Vicker's hardness of a variety of crystalline metals, insulators and semiconductors. The Chen's model is given as:

$$Hv = 2\left(\frac{G^3}{B^2}\right)^{0.585} - 3. \quad (15)$$

Where G and B are shear and bulk modulus respectively. The Vicker's hardness of BP₃N₆ is given in Table V. Clearly, BP₃N₆ has high Vicker's hardness close to that of Pnnm-CN and hence a potential superhard material. The strong resistance to change in volume and shape as

TABLE IV. bulk modulus (B), shear modulus (G), Young's modulus (E), and Poissons ratio (n) of BP_3N_6 in Hills', Voigt's and Reuss's approaches.

Pressure	Bulk modulus (GPa)			Young's modulus (GPa)			Shear modulus (GPa)			Poisson's ratio		
	B_V	B_R	B	E_V	E_R	E	G_V	G_R	G	n_V	n_R	n
0	330.9	330.5	330.7	716.8	713.5	715.2	314.6	312.8	313.7	0.13897	0.14026	0.13961
20	424.6	424.3	424.4	853.9	851.4	852.6	366.5	365.2	365.9	0.16485	0.16557	0.16521
42.4	505.2	504.9	505.1	967.7	965.6	966.6	409.7	408.7	409.2	0.18077	0.18129	0.18103

TABLE V. The shear anisotropy factors ($A_{\{100\}}, A_{\{010\}}, A_{\{001\}}$), percent anisotropy factors of bulk (A_B) and shear (A_G) moduli, universal anisotropy factor A^U , G/B ratio, Knoop hardness and Vickers hardness (H_v) in GPa calculated for BP_3N_6 using PBE functionals.

	Pressure	$A_{\{100\}}$	$A_{\{010\}}$	$A_{\{001\}}$	A_B	A_G	A^U	G/B	H_v
BP_3N_6	0	0.82	0.98	0.91	0.05	0.287	0.02	0.94	51.2
	20	0.85	1.01	0.96	0.03	0.170	0.01	0.86	50.1
	42.4	0.87	1.03	1.00	0.02	0.120	0.01	0.81	49.7

a result of highly condensed orthorhombic structure explains this unexpected behavior in BP_3N_6 . Right from large elastic constants to large bulk and shear moduli, to small values of Poisson's ratio (ν) and large Vicker's harness, BP_3N_6 portray similar behaviour to well known superhard materials. However, pressure frustrates the hardness of BP_3N_6 .

IV. CONCLUSION

BP_3N_6 has been investigated at different pressure starting from zero pressure to a maximum of 42.4 GPa. Clearly, the high value of bulk modulus indicate that BP_3N_6 is a low compressible material. This character emanates from the highly condensed orthorhombic structure built up from the tetrahedra BN_4 and octahedra PN_6 coordination. A comprehensive analysis of elastic constants and its derived properties beside bulk mod-

ulus have been presented. BP_3N_6 displays high resistance to change in shape which greatly contributes to its high Vicker's hardness of about 51 GPa at zero pressure. Overall, BP_3N_6 has similar behavior as those of well known superhard materials and hence the conclusion that BP_3N_6 is a potential superhard material. These results provides guidance for further exploration of thermodynamic stability and many other properties of BP_3N_6 at different pressures.

ACKNOWLEDGMENTS

This work was financially supported by Kenya Education Network (KENET) through Computational Modeling and Materials Science (CMMS) Research mini-grants 2019. We acknowledge the Centre for High Performance Computing (CHPC), Cape Town, South Africa, for providing us with computing facilities.

* gmanyali@mmust.ac.ke

¹ Lyakhov, Andriy O., and Artem R. Oganov., Phys. Rev. B **84**, 9, (2011), 092103.

² Tang, Xiao, Jian Hao, and Yinwei Li., Physical Chemistry Chemical Physics **17**, 41, (2015), 27821-27825.

³ Manyali, George S, Ab-initio study of elastic and structural properties of layered nitride materials, University of the Witwatersrand, Johannesburg, (2012).

⁴ Manyali George S and Warmbier, Robert and Quandt, Alexander and Lowther, John E, Comput. Mater. Sci., **69**, (2013) 299–303.

⁵ Manyali, George S and Warmbier, Robert and Quandt, Alexander, Comput. Mater. Sci., **79**, (2013) 710–714.

⁶ G. S. Manyali, R. Warmbier and A. Quandt, Comput. Mater. Sci. **96**, (2015) 140-145.

⁷ Vogel, Sebastian, Amalina T. Buda, and Wolfgang Schnick., Angewandte Chemie International Edition **57**, no. 40 (2018): 13202-13205.

⁸ Vogel, Sebastian *et.al* Angewandte Chemie International Edition, (2019).

⁹ P. Hohenberg and W. Kohn, Phys. Rev. **136**, (1964), B864.

¹⁰ Kohn, Walter and Sham, Lu Jeu, Phys. Rev., **140**, 4A, (1965) A1133.

¹¹ J. P. Perdew, K. Burke, and M. Ernzerhof, Phys. Rev. Lett. **77**, 3865 (1996).

¹² Giannozzi, Paolo *et.al*, Journal of physics: Condensed matter, **21**, 39, (2009) 395502.

¹³ Dal Corso, Andrea, Comput. Mater. Sci., **95**, (2014), 337–350.

¹⁴ H. J. Monkhorst and J. D. Pack, Phys. Rev. B **13**, 5188 (1976).

- ¹⁵ Corso, Andrea, *Journal of Physics: Condensed Matter*, **28**, 7, (2016), 075401.
- ¹⁶ Palumbo, Mauro and Dal Corso, Andrea, *physica status solidi (b)*, **254**, 9, (2017)
- ¹⁷ F. D. Murnaghan, *Proc. Natl. Acad. Sci. USA* 30, 244 (1944).
- ¹⁸ Born, Max and Kun Huang, *Dynamical theory of crystal*, (Clarendon press, 1954)
- ¹⁹ Mouhat, Felix, and Francois-Xavier Coudert. *Phys. Rev. B* **90**, 22 (2014), 224104.
- ²⁰ Ravindran, P and Fast, Lars and Korzhavyi, P A_ and Johansson, B and Wills, J and Eriksson, O, *Journal of Applied Physics*, **84**, (1998) 4891–4904.
- ²¹ Wen, Yufeng, Long Wang, Huilong Liu, and Lin Song, *Crystals* **7**, 2 (2017) 39.
- ²² Voigt, Woldemar. *Lehrbuch der kristallphysik*. **962** Leipzig: Teubner, 1928.
- ²³ Reuss, A., *Angew. Z. Berechnung del fliessgrenze von mischkristallen auf grund der plastizitatbedingung for einkristalle*. *Math. Mech.* **9**,(1929), 4958.
- ²⁴ Hill, R. The elastic behaviour of a crystalline aggregate. *Proc. Phys. Soc. A*, **65** (1953), 349354.
- ²⁵ J. Haines, J.M. Leger, G. Bocquillon, *Annual Review of Materials Research* **31**, 1, (2001) 123
- ²⁶ S.F. Pugh. 1954 *Philos. Mag.* **45** 823843.
- ²⁷ H.Y. Chung, M.B. Weinberger, J.M. Yang, S.H. Tolbert, R.B. Kaner, *Appl. Phys. Lett.* **92**, (2008) 261904.
- ²⁸ R.A. Andrievskiy, in: *Proceeding of the Seventeenth International Offshore and Polar Engineering Conference*, (2007).
- ²⁹ C. Doughty, S.M. Gorbalkin, T.Y. Tsui, G.M. Pharr, D.L. Medlin, *J. Vac. Sci. Technol. A* **15** (1997) 2623.
- ³⁰ Chen, Xing-Qiu and Niu, Haiyang and Li, Dianzhong and Li, Yiyi, *Intermetallics*, **19**, (2011) 1275–1281.
- ³¹ Chung, DH and Buessem, WR, *Journal of Applied Physics*, **38**, (1967), 2010–2012.
- ³² Ranganathan, Shivakumar I and Ostojca-Starzewski, Martin, *Phys. Rev. Lett.*, **101**, (2008) 055504.